

Exploring the Etiology of Pelvic Organ Prolapse with Finite Element Analysis

A Technical Report submitted to the Department of Biomedical Engineering

Presented to the Faculty of the School of Engineering and Applied Science
University of Virginia • Charlottesville, Virginia

In Partial Fulfillment of the Requirements for the Degree
Bachelor of Science, School of Engineering

Olivia Mergler

Spring, 2024

Word Count: 4747

Number of Figures and Tables: 14


Number of Equations: 0

Number of Supplements: 0

Number of References: 33

On my honor as a University Student, I have neither given nor received unauthorized aid on this assignment as defined by the Honor Guidelines for Thesis-Related Assignments

William Guilford, Department of Biomedical Engineering

Signed  Date 5/6/2024
Olivia Mergler

Approved  Date 5/6/2024
William Guilford, Department of Biomedical Engineering

Exploring the Etiology of Pelvic Organ Prolapse with Finite Element Analysis

Olivia R. Mergler^a, William H. Guilford^a

^a Department of Biomedical Engineering, University of Virginia

Abstract

Pelvic organ prolapse (POP) is caused by the descent of the pelvic organs into the vaginal wall, leading to discomfort, urinary and fecal incontinence, and reduced mental and sexual health of approximately 41% of post-menopausal women. Despite the widespread burden of POP, treatment options have excessively high failure rates. To improve POP treatment options, it is important to better understand where support reinforcement is necessary to correct the prolapse, requiring investigation of the biomechanical changes that cause POP. This Capstone project aimed to develop a biofidelic computational model of the female pelvic floor to explore the effects of specific pelvic floor support impairments on pelvic floor morphology. Through this project, a model of a healthy pelvic floor during the Valsalva maneuver was developed, capturing clinically observed deformations such as descent of the cervix and vagina, compression of the rectum, and bulging of the perineal body during increases in intraabdominal pressure. Impairments of the vaginal wall, rectovaginal fascia, levator ani muscle, pelvic floor muscles (bulbocavernosus, ischioavernosus, and perineal muscles), perineal body, and reproductive ligaments were simulated through a reduction of their associated stiffnesses. Impairment of the reproductive ligaments and levator ani muscle resulted in increased cervical descent. Distal vaginal wall descent was associated with levator ani, vaginal wall, reproductive ligament, and pelvic floor muscle impairment. Weakening of the vaginal wall also led to widening of the vaginal introitus. Each of these deformation modes were exacerbated upon execution of simulations that captured combinations of impairments. This model progresses the understanding of the discrete roles of pelvic floor support structures and offers a method to continue exploration of diverse pelvic floor disorders.

Keywords: Computational modeling, pelvic organ prolapse, finite element analysis, women's health

Introduction

Pelvic organ prolapse (POP) is the herniation of pelvic organs (rectum, uterus, or bladder) into the vaginal wall. This condition is present in approximately 41% of post-menopausal women, resulting in an 11-19% lifetime risk of undergoing prolapse or incontinence surgery¹. Although treatment with surgeries and pessaries is abundant, approximately 30% of surgeries to correct prolapse fail, and pessaries are not effective in relieving symptoms of 42% of those who experience POP^{1,2}. POP can cause negative effects on patients' health-related quality of life, including causing uncomfortable pressures in the vagina, urinary and fecal incontinence, and deterioration of mental and sexual health, necessitating the development of more effective treatment options^{3,4}. To begin to improve current treatment options, a better understanding of the underlying mechanics of POP is necessary.

Pelvic Floor Anatomy

A basic understanding of the functions of healthy pelvic floor supports exists through investigations of structural and functional differences between women with and without prolapse using magnetic resonance imaging (MRI), ultrasound, and functional pelvic floor testing. Through these tests, a collection of structural interactions has been observed, advancing the understanding of the roles of the connective tissue and muscles that support the pelvic floor. Four main impairments have been identified to contribute to prolapse: impairments to the pelvic floor muscles, the reproductive ligaments, the rectovaginal fascia, and the vaginal wall.

The pelvic floor muscles serve to lift and close the vagina. When these muscles are functional, the vagina maintains intra-abdominal pressure, reducing the pressure differential between the vagina and the abdomen and rectum to reduce strain on the vaginal wall⁵. However, if the pelvic floor muscles are impaired (particularly the bulbocavernosus muscle) due

to injury or neurological damage, the vaginal introitus can open, causing a dysregulation of the pressure gradient and subsequent descent of the pelvic organs into the vaginal wall^{5,6}. This pressure gradient can also perpetuate increased strain on the rectovaginal fascia, causing it to weaken and even tear upon repeated loadings⁷. Furthermore, the reproductive ligaments, particularly the cardinal and uterosacral ligaments, serve to suspend the vagina and uterus. However, it has been found that in prolapse patients, these ligaments are longer at rest and stretch significantly more during increases in intra-abdominal pressure, allowing for greater mobility of the vagina upon pressure application⁸. Material changes in the vaginal wall and rectovaginal fascia are also commonly cited theories of prolapse pathology. Some studies show that tissue samples of the vaginal wall of prolapse patients exhibit reduced smooth muscle compositions, possibly associated with increased rates of apoptosis^{9,10}. Alterations in connective tissue compositions, such as reduced elastin expression have also been noted, though these results are inconsistent throughout literature¹¹. Lastly, weakening of the perineal body has been found to cause increased perineal descent, enabling posterior vaginal prolapse¹².

Such impairments have been assigned risk factors including postmenopausal age, parity, obesity, hysterectomy, or chronic coughing¹. These conditions have been associated with trauma to the support structures and/or chronic loading that causes tissue detachment, fatigue, and/or remodeling¹. Overall, it is evident that prolapse is likely caused by a complex collection of biomechanical changes. Although these impairments have been found to cause prolapse, continued work remains necessary to understand the support failures associated with specific morphological changes. This progress will facilitate the development of improved treatment options by enabling identification of the specific support repairs necessary for different prolapse types.

Prolapse and Finite Element Analysis

Finite element analysis provides the opportunity to non-invasively explore complex biomechanics through simulating interactions between the relevant anatomy¹³. Computational biomechanical models have been introduced to the women’s health field to better understand pelvic floor dynamics, especially during pregnancy and pelvic floor disorders¹⁴⁻¹⁶. Due to the low cost of resources to produce, computational models have the potential to be designed with vast variability in subject anatomy and pathological conditions, enabling an in-depth understanding of the effects of discrete changes of mechanical properties that is not attainable with human studies.

Current FE models of POP typically rely upon MRIs for model construction and are subsequently used to investigate the functionality of specific support systems. These models have predominantly explored the role of the levator ani muscle and reproductive ligaments on prolapse morphologies. For example, Luo et al. developed an FE model including the anterior and posterior vaginal wall and adjacent support structures. This model identified that impairments to support structures such as the levator ani and reproductive ligaments can predictably lead to anterior or posterior vaginal wall descent¹⁷. Chen et al. developed a simplified 3D biomechanical model based on MRIs to understand the support impairments that contribute to anterior vaginal prolapse. They determined that impairment of the pubovisceral muscle and cardinal ligaments were the most influential in anterior vaginal prolapse¹⁸. Babayi et al. conducted a parametric analysis to understand the role of soft tissue and ligament impairments on pelvic floor displacements by modeling pelvic floor anatomy as beam and rod elements. They found that increased intra-abdominal pressure and deterioration of the pelvic floor muscle passive strength were associated with increased prolapse severity¹⁹.

Biofidelic computational models of the pelvic floor have been developed to explore pelvic floor kinematics. These models are more computationally expensive and require a complex model development process for each subject, making them impractical for patient-specific clinical diagnostics. However, they can improve the accuracy of the model response by limiting simplification of the geometry. Dias et al. developed a model of the female pelvic floor including the pelvic bones, organs, levator ani, fat, and a “bodyfill” that represents intra-abdominal

components¹⁴. The authors’ development of a bodyfill improves model biofidelity by simulating dissipation of intra-abdominal pressures to the organs, as well as serving as contact surfaces for the anatomy to compress against. A similar model configuration will be used in this study.

This capstone will continue the investigation of the role of the diverse pelvic floor support impairments on pelvic floor deformations associated with prolapse through 1) the development of a healthy pelvic floor model during the Valsalva maneuver, and 2) using the model to simulate support impairments to identify the support failures most influential in POP pathology. In addition to continuing exploration of previously researched support impairments such as that of the levator ani muscle and reproductive ligaments, this work will also include impairments of distal pelvic floor muscles (deep and superficial perineal muscle, ischioavernosus, and bulbocavernosus), the perineal body, and the rectovaginal fascia using a biofidelic model. Based on previous models and clinical findings, it is hypothesized that impairment of the reproductive ligaments will result in loss of apical support of the vagina, while impairment of the levator ani muscles will lead to both a loss of apical support and distal descent of the vaginal wall. Impairment of the vaginal wall and rectovaginal fascia will enable greater laxity and protrusion of the pelvic organs into the vaginal wall.

Results

Geometry Definition

Following segmentation, smoothing, and meshing of the model geometry, the complete model consisted of 25 biofidelic tissue components and 356,524 tetrahedral mesh elements (Figure 1).

Model Tuning

The initial model geometry included bowel superior to the uterus. However, it was observed that the bowel reduced the compression of the inferiorly positioned organs, such as the uterus and rectum. It appeared that the deformability of the internal contents of the bowel was not adequately captured during the simulations, constraining the ability for the bowel to compress and be displaced upon pressure application. To better capture the uniform compression due to increased intra-abdominal

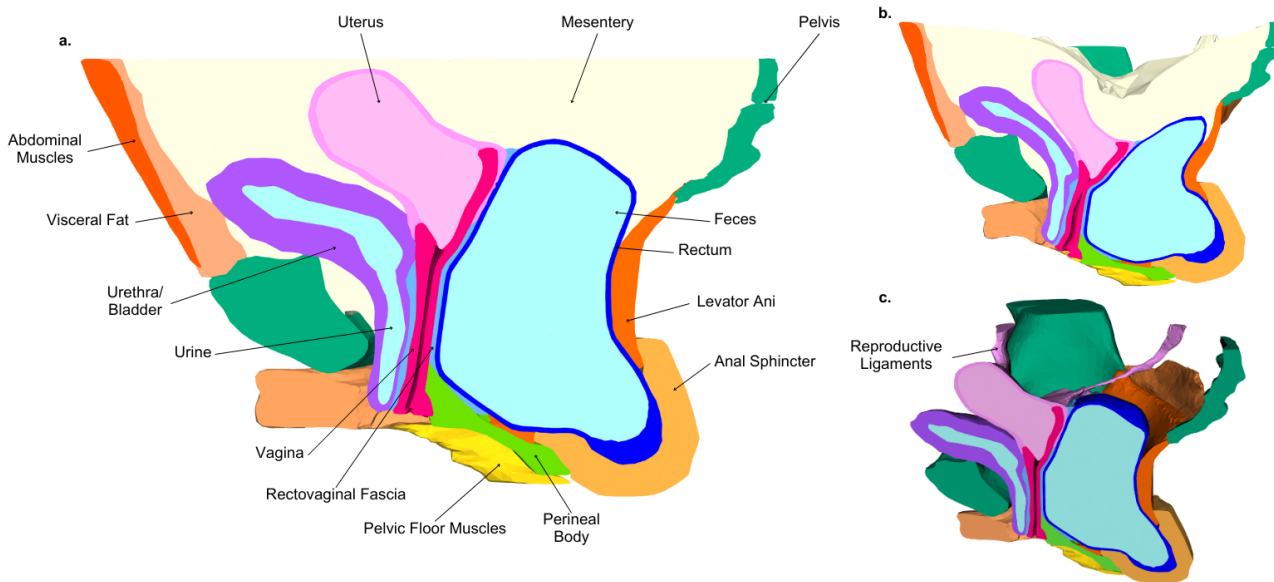


Figure 1: Complete healthy model assembly a) at rest, b) at maximum Valsalva maneuver, and c) at rest with mesentery removed for organ visualization.

pressure, the bowel was removed, and the gaps were filled in with mesentery. Doing so improved the response of the organs compared to imaging observations, specifically demonstrating increased compression and displacement of the uterus, bladder, and rectum.

To continue to improve the biofidelic response of model, particularly of the compression of the rectum and bladder during the Valsalva maneuver, the material properties of the mesentery were tuned. Currently, the most comprehensive characterization of this material was modeled with an elastic modulus of 5 MPa¹⁴. However, this resulted in limited deformation of the pelvic organs, thus, the material property was iteratively reduced between 5 MPa and 0.1 MPa. Additionally, due to limited visibility of the reproductive ligaments in the VH cryosections, boundaries were based upon the Anatomage table outlines. However, due to the resolution of the cryosections and approximations of boundaries, the ligaments were ultimately thicker than what is anatomically accurate. For example, the uterosacral ligament is typically approximately 4.4 mm thick, while some portions of the segmented ligament exceed 12 mm²⁰. Consequently, the reproductive ligament material properties were reduced to account for this excessive thickness to generate a stiffness representative of the true ligaments. Several iterations were tested, ranging from 14 MPa (experimentally determined modulus), to 0.001 MPa²¹.

Several combinations of mesentery and ligament material properties were presented to Dr. Vaughan, a gynecologist at the UVA Health center. It was concluded that 0.5 MPa and 0.01 MPa were the optimal elastic moduli for the mesentery and reproductive ligaments, respectively to enable the organ compression and cervical descent representative of a healthy patient.

Model Validation

To confirm the model accuracy compared to deformations expected clinically, measurements of cervical, rectal, and perineal body descent were compared to published observations (Table 1). Each of the measured criteria fell within the expected range, demonstrating an appropriate model response during the Valsalva maneuver.

Table 1: Quantitative comparison of model deformations to clinical measurements of healthy patients during Valsalva maneuver.

Deformation	Expected Range (cm)	Measured Displacement (cm)
Cervical Descent	0 to 5.9 ²²	1.6
Rectal Protrusion	< 1 cm ²³	0.2
Perineum Descent	< 3 cm ²⁴	0.8

Furthermore, observations of morphological changes were compared to MRIs of healthy patients during the Valsalva maneuver. Deformations such as posterior tilt of the vaginal wall and uterus, descent of the pelvic floor, and compression of the rectum were markers of realistic resulting deformations (Figure 2).

Impairment Simulations

During POP, large deformations occur, such as “kneeling” of the vaginal wall, protrusion of the rectum or bladder into the vaginal walls, descent of the cervix towards the genital hiatus, and protrusion of the vaginal wall out of the genital hiatus. Unfortunately, this model was unable to capture these dramatic deformations, as the resulting displacements of the organs were on the scale of a few millimeters. However, the deformations that resulted from the simulations do demonstrate morphological changes that have been reported to prelude prolapse. Four main different deformation modes were found: 1) cervical descent, 2) widening of the vaginal introitus, 3) descent of the distal vaginal walls, and 4) change in angle of

the vagina. Each of these changes were associated with one or few impairment states that may be used to elucidate the etiology of different pelvic floor morphological changes (Figure 3).

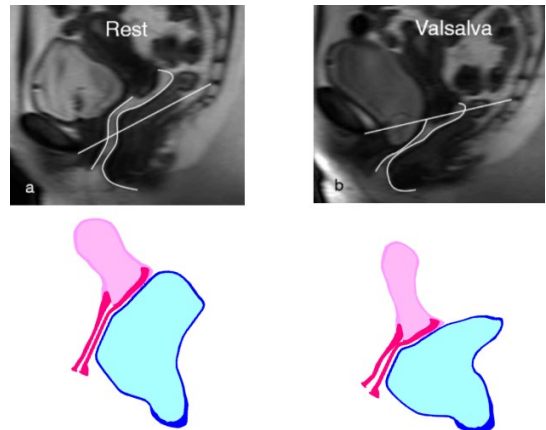


Figure 2: Qualitative comparison of model deformations to MRIs of healthy pelvic floor during Valsalva maneuver. MRIs from Liu et al.²⁵

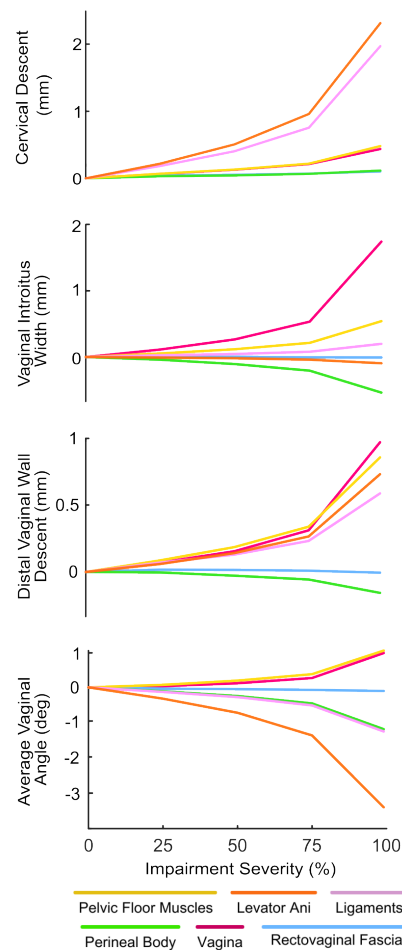


Figure 3: Plots of vaginal deformations during discrete impairment states. All deformations are measured relative to the healthy model during maximum Valsalva maneuver.

Cervical Descent

Impairment of the reproductive ligaments and levator ani muscle were associated with increased descent of the cervix. Impairment of the levator ani muscle enabled posterior and inferior deformation of the superior portion of the rectum (Figure 4). This displacement caused the vagina and uterus to also tilt posteriorly, resulting in descent of the uterus.

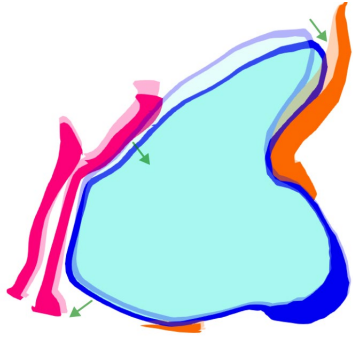


Figure 4: Deformation of rectum and vagina in healthy (lighter) and levator ani impairment (darker) state.

Alternatively, impairment of the reproductive ligaments caused minimal changes to the rectum, and instead enabled the uterus and vagina to sag primarily downwards rather than tilting posteriorly (Figure 5). A simulation of ligament avulsion, rather than simply weakening of the material properties was also conducted, resulting in a 62% greater descent of the cervix than the maximum impairment state.

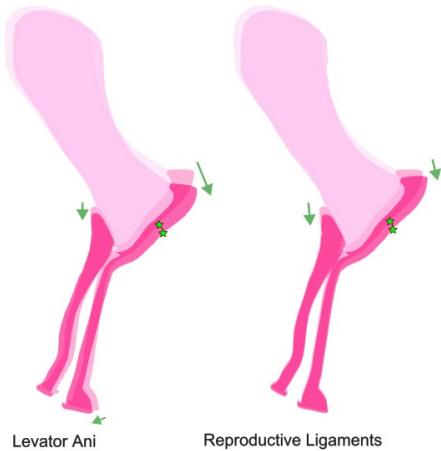


Figure 5: Comparison of cervical descent in levator ani and reproductive ligament impairment states.

Vaginal Introitus Widening

Impairment to the vaginal wall was most associated with midvaginal and vaginal introitus widening. The weakening of the vaginal walls enabled outward displacement of both the anterior and posterior vaginal walls and minor sagging of the superior vaginal walls. Alternatively, weakening of the perineal body enabled closing of the vaginal walls. In a healthy state, the perineal body constrained the motion of the posterior vaginal wall. Upon weakening, the perineal body stretched more, enabling the posterior vaginal wall to move anteriorly with the anterior vaginal wall, reducing the gap size between the walls (Figure 6).

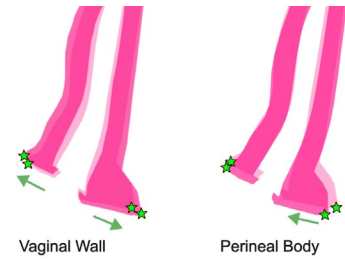


Figure 6: Comparison of vaginal widening in vaginal wall and perineal body impairment states.

Vaginal Wall Descent

The descent of the vaginal walls was associated with impairment of the vaginal wall, pelvic floor muscles, levator ani muscle, and reproductive ligaments (Figure 7). Impairment of the vaginal wall caused the greatest descent due to both sagging of the walls, and the ability for the posterior vaginal wall to be stretched posteriorly and inferiorly by the adjacent perineal body. As previously discussed, the weakening of the levator ani muscle enabled posterior and inferior compression of the superior portion of the rectum. This deformation resulted in protrusion of the distal portion of the rectum into the perineal body, causing the remainder of the pelvic floor to descend and tilt anteriorly. During impairment of the pelvic floor muscles, this anterior tilt of the pelvic floor was absent. Rather, the pelvic floor displaced downwards with a slight posterior shift. The reproductive ligaments enabled the vagina to tilt posteriorly, causing descent of the posterior vaginal wall.

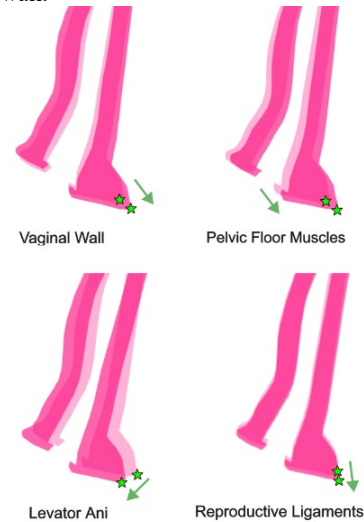


Figure 7: Comparison of distal vaginal descent in vaginal wall, pelvic floor muscle, levator ani and reproductive ligament impairment states.

Vaginal Angle

Impairment of the levator ani muscle resulted in increased posterior tilt of the vaginal walls due to the backwards displacement of the rectum previously discussed. Similarly, weakening of the reproductive ligaments enabled a posterior shift of the uterus and apical portion of the vagina, reducing the average vaginal angle (Figure 8). Impairment of the pelvic floor muscles caused a more vertical position of the vaginal walls as the distal portion of the vagina descended and shifted posteriorly.

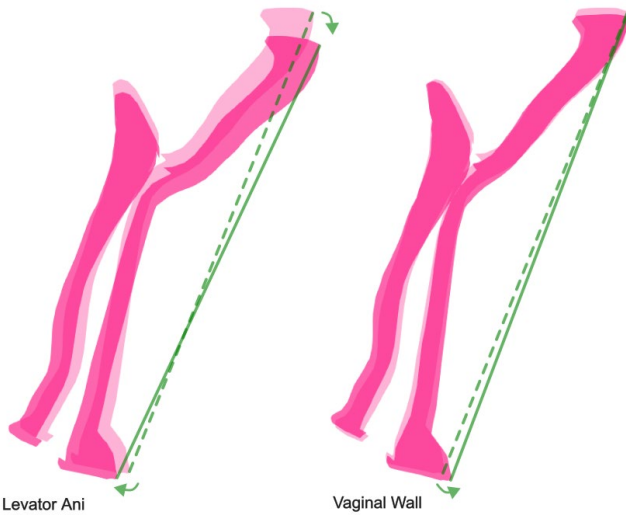


Figure 8: Comparison of vaginal angle in levator ani and vaginal wall impairment states.

Combination Simulation

Combinations of impairments resulted in increased cervical descent, vaginal widening, and vaginal wall descent and demonstrated the likelihood of multiple deformation modes occurring simultaneously (Figure 9, Table 2). For example, in a simulation combining levator ani and reproductive ligament impairments, both the cervical descent and distal vaginal wall descent increased. Similarly, although impairment of the vaginal wall had a considerably greater effects on vaginal width than any other impairment type, when impairment of pelvic floor muscles and vaginal wall were combined, the hiatus width increased 34% more than with a vaginal wall impairment alone. A combination of impairments of the pelvic floor muscles, levator ani, vaginal wall, and reproductive ligaments resulted in increased deformation of all three modes. The change in vaginal angle during the full combination simulation did not exceed the change in magnitude observed in the levator ani simulation. This is due to the posterior-inferior descent of both the distal and superior vagina, limiting the overall change in angle.

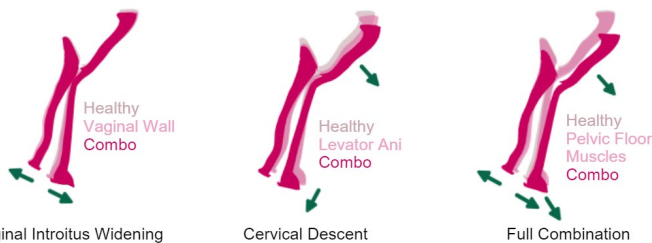


Figure 9: Visualization of comparison of deformation magnitudes in discrete impairment states and combination states. See Table 4 for combination simulation descriptions.

Discussion

This study provided insight on the mechanical role of different support structures and their potential contribution to prolapse upon impairment. Several observations confirmed the hypothesized deformations and were consistent with previous models and clinical findings. For example, impairments of the levator ani muscle have frequently been modeled and found to be associated with increased prolapse severity^{18,26}.

Table 2: Quantification of comparison of deformation magnitudes in discrete impairment states and combination states.

Combination Simulation	Max Discrete Deformation (associated impairment)	Combination Deformation
Cervical Descent (mm)	2.4 (levator ani)	4.2
Vaginal Widening (mm)	1.7 (vaginal wall)	2.4
Full Combination		
Vaginal Wall Descent (mm)	1.0 (vaginal wall)	3.0
Cervical Descent (mm)	2.4 (levator ani)	5.6
Vaginal Widening (mm)	1.7 (vaginal wall)	2.7
Vaginal Angle (deg)	-3.3 (levator ani)	-2.8

This model captured the descent of the distal vaginal wall due to the reduction of the passive properties of the muscles that has been previously reported in literature¹⁹. Existing models and clinical findings have also identified the role of apical support from the levator ani muscle^{8,18}. This support from the levator ani muscle was apparent in this model through its effect on cervical descent upon impairment. Previous models have reported mixed conclusions on the contribution of the ligaments in prolapse morphologies, however clinical observations have consistently attributed ligament weakening, lengthening, or detachment to increased prolapse severity^{18,19}. This model captured a distinguished role of the reproductive ligaments in cervical descent, corroborating with the clinical observations. The findings of this model may also contribute to understanding of the role of relatively understudied pelvic floor support structures. Although many models have explored the role of the levator ani for vaginal wall support, no models were found that investigate the role of the distal pelvic floor muscles in prolapse. Although this model was unable to capture the sealing effects of the pelvic floor muscles, the impairment simulations did demonstrate their role in mechanically lifting the distal vagina. Interestingly, although rectovaginal fascia weakening has been thought to cause posterior vaginal prolapse, impairment of the rectovaginal fascia had no measurable effect on the pelvic floor displacements²⁷. Lastly, laxity of the vaginal wall has been hypothesized to cause increased herniation of the pelvic organs²⁸. This model demonstrates that weakening of the vaginal wall can also be associated with widening of the cavity, which has been found clinically to prelude apical/ cervical prolapse, as well as vaginal wall descent²⁹.

The development of this model enables continued exploration of pelvic floor biomechanics in prolapse scenarios, as well as in conditions such as stress urinary incontinence and defecatory disorders, injury states including tearing of the pubovisceral muscle or perineal body after childbirth, or dramatic pelvic floor changes such as a following a hysterectomy. By continuing to understand the fundamental biomechanical changes that prelude or follow these conditions, improvements can be made to the prediction, prevention, and treatment of pelvic floor disorders.

Limitations

Although this model provides insight into the support failures contributing to POP, the deformations resulting from impairment simulations do not adequately capture the displacements seen in prolapse. The displacements found in each mode are on the scale of millimeters, whereas the deformations during prolapse are often considered severe when they exceed several centimeters. For example, cervical descent in the impairment simulations did not exceed 3 mm at 99% impairment. A mild case of prolapse is defined when the cervix descends to 1 cm above the vaginal hiatus and becomes severe when it becomes exposed outside

of the hiatus. In the current model, the cervix at its maximal descent is still 6 cm above the vaginal hiatus. This limited degree of deformation was found in each impairment mode.

To continue to explore the potential of this model in investigating pelvic floor dysfunction, it is important to improve the biofidelity of the model. First steps should include modifying the contact conditions of the model to more accurately represent interactions between tissues. Currently, all contacts are defined as rigid between each tissue component. While many adhesions exist in the pelvic floor, such as between the levator ani and the bony pelvis, sliding interactions often exist between organs. For example, the vagina and bladder move largely independently, which would be best represented by a frictional contact.

Additionally, this model is limited due to it capturing a single patient geometry. It has been hypothesized that variations such as ligament length or bony pelvis dimensions may predispose women to prolapse due to increased ability to deform and a larger area for application of intraabdominal pressure³⁰. To create a comprehensive understanding of the role of support impairments in prolapse morphologies, it is important to continue to develop models on diverse geometries. The Korean Visible Human database offers two additional open-source female models, however, clinical collaboration to access MRIs would enable a more robust inventory of potential model geometries.

Lastly, the material characterization of the tissues is limited by lacking and inconsistent models defined in literature. For example, in literature, the rectum elastic modulus ranges from approximately equal to that of the vagina to over 20 times stiffer^{14,25}. Material characterization of the distal pelvic floor muscles were entirely absent, requiring the assumption that they behaved similarly to the levator ani muscles. Therefore, many approximations were made when defining Ogden model material parameters.

Materials and Methods

Model development consisted of geometry segmentation, smoothing, and meshing, simulation design and tuning, and concluded with the execution of impairment simulations (Figure 10).

Model Geometry Development

Model geometry was developed through segmentation of cryosections from the National Library of Medicine's female Visible Human Project, an open-source 3D representation of a healthy female cadaver (Figure 10a). The cryosections were taken in 0.33 mm intervals, enabling high resolution of the subject for reconstruction, with greater visible details necessary to differentiate between tissues and muscle groups than computed tomography or MRI. Tissue segmentations were created through slice-by-slice manual "painting" of the anatomy using 3D Slicer. Tissue boundaries were informed using the Anatomage Table interactive 3D anatomy visualization that outlined anatomy using the female Visible Human cryosections. All tissue components were extended to include adjacent connective tissue associated with the component to ensure continuous contact between all bodies.

These segmentations were used to create components of the organs, muscles, mesentery, fat, bones, and ligaments of the pelvic floor. The tissues began at the level of the vaginal introitus and ended just above the top of the uterus. Using ANSYS SpaceClaim, the raw segmentations were converted to faceted bodies, reduced, and smoothed to create simplified geometries of each tissue component. (Figure 10b).

The final model was converted to a constructive solid geometry (CSG) and used to create an adaptive tetrahedral mesh using fTetMesh, an open-source GitHub software (Figure 10c).

Healthy Simulation Design

Simulations of a healthy pelvic floor were designed to capture the material properties and boundary conditions relevant to the local anatomy (Figure 10d). Gravity was applied to assume a standing posture of the model. The model was rigidly constrained on the top of the pelvis and coccyx. To represent the increased intra-abdominal pressure as a result of the Valsalva maneuver in the model, a graded pressure of 120 cmH₂O was applied to the top surface of the model¹⁴. Additionally, the same pressure

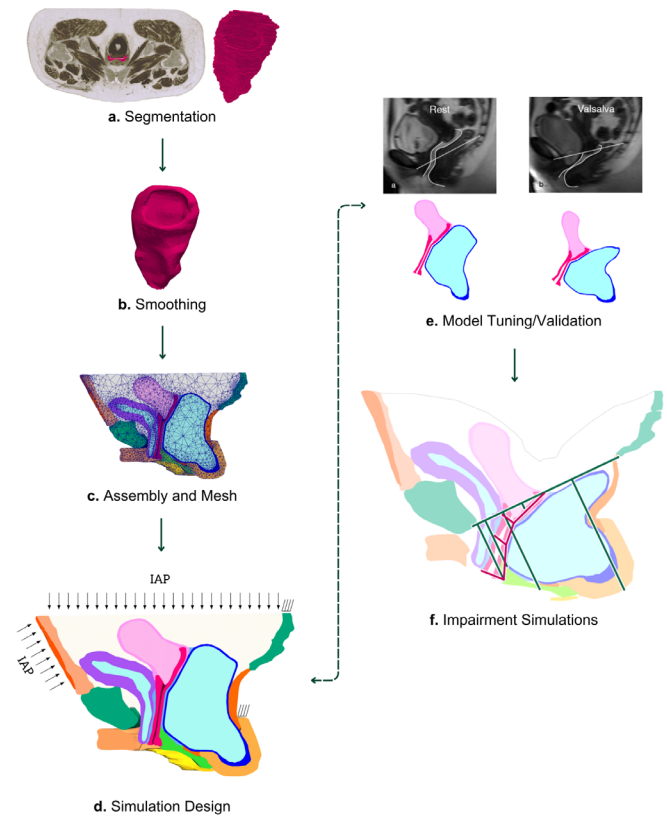


Figure 10: Overview of model development and simulation design methods.

grading was applied to the anterior surface of the abdominal muscles to represent the pressure due to their contraction. The exposed ends of the reproductive ligaments at the top of the model were fixed to capture their adhesion to the pelvis beyond the boundaries of the model. Lastly, the superior-posterior surface of the anal sphincter was rigidly constrained to simulate the restraining effect of the anococcygeal ligament.

Soft tissues exhibit hyperelastic material properties and large deformation during prolapse. To adequately capture these properties, an incompressible Ogden material model was used to characterize most of the pelvic floor anatomy. Materials that underwent small deformations or were less structurally relevant were modeled with a Neo-Hookean material to reduce computational times. Due to limited characterization of pelvic floor tissues using an Ogden model, the material parameters were linearly scaled between tissues based on published elastic moduli (referenced moduli in Table 3). The levator ani and pelvic floor muscles were represented in a contracted state, associated with an increased elastic modulus³¹. Material properties of the mesentery and reproductive ligaments were tuned to capture deformations representative of a healthy pelvic floor during Valsalva (Figure 10e).

These simulations were designed using PolyFEM, an open-source GitHub finite element library, and a Houdini user interface for element selection used in boundary condition applications. The simulations were scaled to one second, using 0.025 second intervals. An Eigen::PardisoLU solver was used due to its ability to solve robust finite element models and use of parallel solving to reduce computational times. To minimize run times, the simulations were executed on Rivanna using 10 cores. Final simulation solve times ranged between 3-28 hours.

Measurements to validate the model deformations were taken as the difference between the point at which the model settled due to gravity, and the end point of the simulation where maximal IAP was applied.

Impairment Simulation Design

Impairments were simulated for the vaginal wall, rectovaginal fascia, reproductive ligaments, levator ani muscles, perineal body, and pelvic floor muscles (Figure 8f). Support impairments were simulated by reducing the material properties of the respective tissues. Four degrees of impairments were evaluated: 25, 50, 75, and 99%. Additionally, reproductive ligament avulsion was simulated by removing the fixed constraints at the top of the ligaments.

Table 3: Elastic moduli used to develop material models for each tissue type. *Tuned based on comparison to MRIs. **Modeled excessively stiff to behave as a rigid body.

Tissue	Elastic Modulus (MPa)
Ogden Material Model	
Vagina	0.015 ²⁵
Rectum	0.011 ²⁵
Urethra	0.015 ²⁵
Uterus	0.003 ³²
Pelvic Floor Muscles	0.031 ³¹
Levator Ani Muscle	0.031 ³¹
Perineal Body	0.029 ²⁵
Reproductive Ligaments	0.001*
Rectovaginal Fascia	0.014 ²⁵
Abdominal Muscle	2.4 ¹⁴
Visceral Fat	0.05 ¹⁴
Neo-Hookean Material Model	
Mesentery	0.035*
Bone	1000**
Poop	0.01 ³³
Urine	0.001 ¹⁴

Measurements

Following simulation, the resulting deformation data was exported, and the node coordinates associated with the following tissue landmarks were recorded: the cervix, anus, center of the perineal body, most anterior point of the rectum, and points marking the distal, mid, and superior posterior and anterior vaginal walls. To measure deformations relative to a rigid reference, a line connecting the most inferior point of the pubic symphysis and the coccyx on the midsagittal plane was created, called the pubococcygeal line. The perpendicular distances of the cervix, anus, anterior rectal wall, and perineal body to the pubococcygeal line were used as metric of the resulting deformations of the pelvic floor. The vertical displacement of the distal posterior vaginal wall was measured as the vaginal wall descent. Points on the vaginal walls were used to quantify the angle and separation width of the walls. All reported measurements were relative to deformations of the healthy model to understand changes in prolapse severity upon support impairments.

Combination Simulations

It is more common clinically for support impairments to occur simultaneously, therefore, combination simulations were designed to understand the impact of multiple support impairments. The impairment types that were most influential in each deformation mode were used in combination, each at 95% impairment. Combination simulations based on the associated deformation mode are described in Table 4.

Table 4: Pelvic floor impairments simulated simultaneously for combination simulations.

Impairment mode	Impaired Structures
Cervical descent	Reproductive ligaments, levator ani muscle
Vaginal Introitus Widening	Vaginal wall, pelvic floor muscles
Full combination	Reproductive ligaments, levator ani muscle, vaginal wall, pelvic floor muscles

End Matter

Author Contributions and Notes

O.R.M created the model, performed simulations, collected data, analyzed the data, and wrote the report. W.H.G. provided advising throughout the project.

The authors declare no conflict of interest.

Acknowledgments

This research was supported by NIH R25 EB023841.

The authors would like to thank:

Dr. Steven Abramowitch for providing guidance in using PolyFEM and fTetWild and help in designing the simulation material characterizations and boundary conditions.

Liam Martin for an introduction to PolyFEM and fTetWild.

Dr. Monique Vaughn for aiding in model tuning.

Dr. Timothy Allen for providing feedback and advising throughout the course.

References

- Rogers, R. G. & Fashokun, T. B. Pelvic organ prolapse in females: Epidemiology, risk factors, clinical manifestations, and management - UpToDate. https://www.uptodate-com.proxy1.library.virginia.edu/contents/pelvic-organ-prolapse-in-females-epidemiology-risk-factors-clinical-manifestations-and-management?search=prolapse&source=search_result&selectedTitle=1~150&usage_type=default&display_rank=1 (2022).
- Manzini, C., van der Vaart, C. H., van den Noort, F., Grob, A. T. M. & Withagen, M. I. J. Pessary fitting for pelvic organ prolapse: parameters associated with specific reasons for failure. *Int. Urogynecology J.* **33**, 2037–2046 (2022).
- Lowder, J. L., Ghatti, C., Nikolajski, C., Oliphant, S. S. & Zyczynski, H. M. Body image perceptions in women with pelvic organ prolapse: a qualitative study. *Am. J. Obstet. Gynecol.* **204**, 441.e1-441.e5 (2011).
- Robinson, D. *et al.* International Urogynaecology Consultation chapter 1 committee 4: patients' perception of disease burden of pelvic organ prolapse. *Int. Urogynecology J.* **33**, 189–210 (2022).
- Shafik, A., Mostafa, R. M., Shafik, A. A. & El-Sibai, O. Study of the effect of straining on the bulbocavernosus muscle with evidence of a straining-bulbocavernosus reflex and its clinical significance. *Int. Urogynecol. J. Pelvic Floor Dysfunct.* **13**, 294–298 (2002).
- Shafik, A., El-Sibai, O., Shafik, A. A. & Ahmed, I. On the pathogenesis of rectocele: the concept of the rectovaginal pressure gradient. *Int. Urogynecology J.* **14**, 310–315 (2003).
- Salvador, J. C., Coutinho, M. P., Venâncio, J. M. & Viamonte, B. Dynamic magnetic resonance imaging of the female pelvic floor—a pictorial review. *Insights Imaging* **10**, 4 (2019).
- DeLancey, J. O. L. What's new in the functional anatomy of pelvic organ prolapse? *Curr. Opin. Obstet. Gynecol.* **28**, 420 (2016).
- Karam, J. A., Vazquez, D. V., Lin, V. K. & Zimmern, P. E. Elastin expression and elastic fibre width in the anterior vaginal wall of postmenopausal women with and without prolapse. *BJU Int.* **100**, 346–350 (2007).
- Takacs, P., Gualtieri, M., Nassiri, M., Candiotti, K. & Medina, Carlos. A. Vaginal smooth muscle cell apoptosis is increased in women with pelvic organ prolapse. *Int. Urogynecology J.* **19**, 1559–1564 (2008).
- De Landsheere, L. *et al.* Histology of the vaginal wall in women with pelvic organ prolapse: a literature review. *Int. Urogynecology J.* **24**, 2011–2020 (2013).

12. Perineal Descent - an overview | ScienceDirect Topics. <https://www.sciencedirect.com/topics/medicine-and-dentistry/perineal-descent>.
13. Sharma, M. & Paul Khurana, S. M. Chapter 17 - Biomedical Engineering: The Recent Trends. in *Omics Technologies and Bio-Engineering* (eds. Barh, D. & Azevedo, V.) 323–336 (Academic Press, 2018). doi:10.1016/B978-0-12-815870-8.00017-6.
14. Dias, N. *et al.* Pelvic floor dynamics during high-impact athletic activities: A computational modeling study. *Clin. Biomech.* **41**, 20–27 (2017).
15. Routzong, M. R., Moalli, P. A., Maiti, S., De Vita, R. & Abramowitch, S. D. Novel simulations to determine the impact of superficial perineal structures on vaginal delivery. *Interface Focus* **9**, 20190011 (2019).
16. Westervelt, A. R. *et al.* A parameterized ultrasound-based finite element analysis of the mechanical environment of pregnancy. *J. Biomech. Eng.* **139**, 051004 (2017).
17. Luo, J., Chen, L., Fenner, D. E., Ashton-Miller, J. A. & DeLancey, J. O. L. A Multi-Compartment 3-D Finite Element Model of Rectocele and Its Interaction with Cystocele. *J. Biomech.* **48**, 1580–1586 (2015).
18. Chen, L., Ashton-Miller, J. A., Hsu, Y. & DeLancey, J. O. L. Interaction Among Apical Support, Levator Ani Impairment, and Anterior Vaginal Wall Prolapse. *Obstet. Gynecol.* **108**, 324 (2006).
19. Babayi, M., Azghani, M.-R., Hajebrahimi, S. & Berghmans, B. Three-dimensional finite element analysis of the pelvic organ prolapse: A parametric biomechanical modeling. *Neurorol. Urodyn.* **38**, 591–598 (2019).
20. Bahar, R. *et al.* OP06.04: Ultrasound evaluation of uterosacral ligament thickness for predicting superficial endometriosis. *Ultrasound Obstet. Gynecol.* **60**, 65–65 (2022).
21. Martins, P. *et al.* Strength of round and uterosacral ligaments: a biomechanical study. *Arch. Gynecol. Obstet.* **287**, 313–318 (2013).
22. Dietz, H. P., Eldridge, A., Grace, M. & Clarke, B. Pelvic organ descent in young nulligravid women. *Am. J. Obstet. Gynecol.* **191**, 95–99 (2004).
23. Arif-Tiwari, H. *et al.* Improved Detection of Pelvic Organ Prolapse: Comparative Utility of Defecography Phase Sequence to Nondefecography Valsalva Maneuvers in Dynamic Pelvic Floor Magnetic Resonance Imaging. *Curr. Probl. Diagn. Radiol.* **48**, 342–347 (2019).
24. Landmann, R. G. & Wexner, S. D. Paradoxical Puborectalis Contraction and Increased Perineal Descent. *Clin. Colon Rectal Surg.* **21**, 138–145 (2008).
25. Liu, X. *et al.* Relationship between high intra-abdominal pressure and compliance of the pelvic floor support system in women without pelvic organ prolapse: A finite element analysis. *Front. Med.* **9**, (2022).
26. Gordon, M. T., DeLancey, J. O. L., Renfro, A., Battles, A. & Chen, L. Development of anatomically based customizable three-dimensional finite-element model of pelvic floor support system: POP-SIM1.0. *Interface Focus* **9**, 20190022 (2019).
27. Posterior vaginal prolapse (rectocele) - Symptoms and causes. *Mayo Clinic* <https://www.mayoclinic.org/diseases-conditions/rectocele/symptoms-causes/syc-20353414>.
28. Meijerink, A. M., van Rijssel, R. H. & van der Linden, P. J. Q. Tissue Composition of the Vaginal Wall in Women with Pelvic Organ Prolapse. *Gynecol. Obstet. Invest.* **75**, 21–27 (2012).
29. Woll, A., Mbaye, M., Edenfield, A. & Swift, S. Genital Hiatus Size as a Predictor of Progression of Pelvic Organ Prolapse. *Urogynecology* **27**, e555 (2021).
30. DeLancey, J. O. *et al.* A unified pelvic floor conceptual model for studying morphological changes with prolapse, age, and parity. *Am. J. Obstet. Gynecol.* **0**, (2023).
31. Tang, J. *et al.* Quantifying Levator Ani Muscle Elasticity Under Normal and Prolapse Conditions by Shear Wave Elastography. *J. Ultrasound Med.* **39**, 1379–1388 (2020).
32. Fang, S. *et al.* Anisotropic Mechanical Properties of the Human Uterus Measured by Spherical Indentation. *Ann. Biomed. Eng.* **49**, 1923–1942 (2021).
33. Yang, P. J., LaMarca, M., Kaminski, C., Chu, D. I. & Hu, D. L. Hydrodynamics of defecation. *Soft Matter* **13**, 4960–4970 (2017).